



Cite this: *RSC Adv.*, 2022, **12**, 35221

Received 7th November 2022  
 Accepted 2nd December 2022

DOI: 10.1039/d2ra07065k  
[rsc.li/rsc-advances](http://rsc.li/rsc-advances)

## 1. Introduction

Organic compounds containing nitrogen are the most important in pharmaceutical molecules and agricultural chemicals. The basic building blocks of life, such as proteins, DNA, and RNA, are nitrogen-containing organic structural units. C–N bonds are found in more than 80% of commonly used medications. In current synthetic chemistry, green and mild methodology for preparing different C–N bonds to replace old harsh preparation protocols is always a hotspot.<sup>1</sup> The technique of *N*-alkylation of amides is well-known, efficient, and essential in the synthesis of natural products, polymers, and peptides.<sup>2–4</sup> Alcohols would be an appropriate option as alkylating reagents for the production of C–N bonds from a green chemistry perspective.<sup>5–13</sup> When compared to other reagents used for *N*-alkylation of amides, alcohols are widely available and relatively inexpensive. *N*-Monoalkylated product is a versatile building block that is commonly utilized in the production of many bioactive compounds<sup>14–17</sup> and pharmaceuticals (Fig. 1).

They are also generally non- or less-toxic and easier to handle. Alcohols, on the other hand, have a poor electrophilicity, required either harsh conditions or further processes. These reactions usually required higher temperatures and/or catalyst loadings, because amides are less nucleophilic than amines. In 2009, Fujita and co-workers developed a method for *N*-alkylation of amides with alcohols using iridium catalysts.<sup>18</sup> Watanabe and Jenner<sup>19,20</sup> and some other researcher<sup>21,22</sup> reported successful use of alcohols as alkylating reagents in the *N*-alkylation of amides using ruthenium and rhodium catalysts at high temperatures. Dean and co-workers reported *N*-

alkylation of amides with alcohols utilizing heterogeneous Ag/Mo oxides in 2011.<sup>23</sup> Alcohols were also reported as alkylating reagents in *N*-alkylation catalyzed by copper,<sup>24</sup> ruthenium,<sup>25</sup> and iridium catalysts<sup>26</sup> in the same year. Sun and coworkers<sup>27</sup> used ruthenium/iridium dual catalyst systems for the alkylation of aldoximes with alcohols to produce *N*-monoalkylated amide. Transition metal based photocatalysts, such as iridium, ruthenium, and polypyridyl complexes, on the other hand, have been associated with numerous of disadvantages, including high cost, low sustainability, and low toughness, possibility of toxicity, as well as being inconvenient during separation.<sup>28–30</sup>

In response to visible light stimulation, the photochemistry of eosin Y has been extensively studied, and it has been discovered that eosin Y undergoes rapid intersystem crossing to the lowest energy triplet state.<sup>31,32</sup> Metal-free organic dyes, particularly eosin Y, were used instead of metal-based photoredox catalysts because they are more cost-effective and environment friendly.<sup>33,34</sup> Visible-light mediated photoredox catalysis for single electron transfer (SET) has emerged in recent years as a viable, versatile, cost-effective, and eco-friendly method for essential chemical transformations such

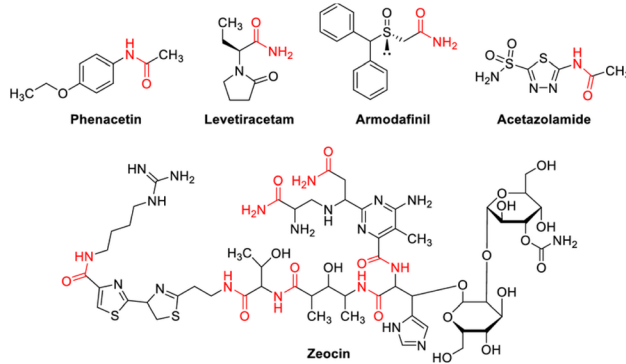
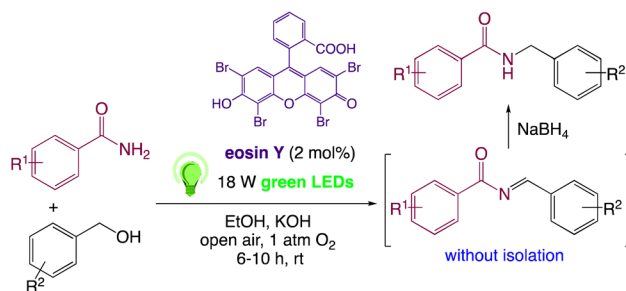


Fig. 1 Some commercially available amide drugs.

<sup>a</sup>Department of Chemistry, CMP Degree College, University of Allahabad, Prayagraj-211002, Uttar Pradesh, India. E-mail: vishalgreenchem@gmail.com

<sup>b</sup>Department of Chemistry, United College of Engineering & Research, Naini, Prayagraj-211010, Uttar Pradesh, India. E-mail: ppssingh23@gmail.com

† Electronic supplementary information (ESI) available. See DOI: <https://doi.org/10.1039/d2ra07065k>



Scheme 1 Photoredox catalyzed C–N coupling of amides with alcohols.

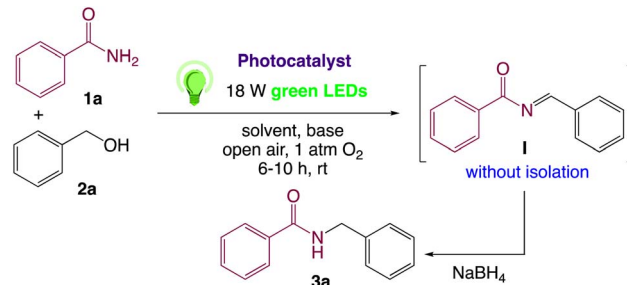
as oxidation/reduction and C–C/C–X bond synthesis in heterocyclic compounds.<sup>35–37a–d</sup> In presence of visible light, an organo-photoredox catalyst has the unique ability to activate air oxygen, a green and natural oxidizing agent, for organic reactions involving SET.<sup>38,39</sup> On the basis of above mentioned previous work, related studies on C–N coupling and in continuation of our work<sup>40–58</sup> on visible light induced photoredox catalysed synthesis, we have proposed eosin Y catalyzed visible-light-induced synthetic protocol for the formation C–N

bond in *N*-monoalkylated product from easily available benzamides and benzyl alcohol (Scheme 1). To the best of our knowledge, this is the first example of photoredox catalysis for the synthesis of *N*-benzylbenzamide. This novel method utilizes visible light photoredox catalysis, which is mechanistically attractive for the production of *N*-monoalkylated product and its derivatives.

## 2. Results and discussion

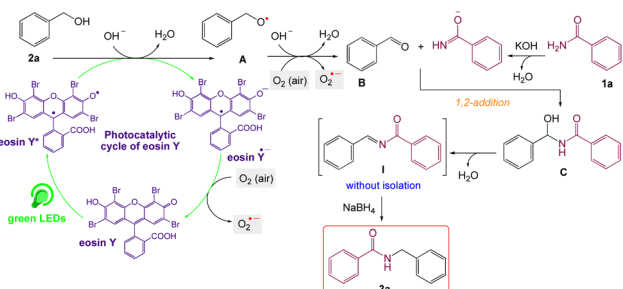
In order to realize our idea and optimize the reaction conditions, the key reaction of benzamide (**1a**) and benzyl alcohol (**2a**), in presence of base with a catalytic amount of eosin Y in a solvent under irradiation with green LEDs [18 W] was carried out (Table 1). By applying several catalysts and bases, we first focused on optimizing the reaction conditions. We were delighted to obtain the desired substituted *N*-monoalkylated product **3a**, in 96% yield (Table 1, entries 1 and 2). Then, the control experiments were carried out, which show that eosin Y, base and visible light are essential for the reaction, because in the absence of any of the reagents/reaction parameters either the product was not detected (n.d.) or was formed in traces (Table 1, entries 2

Table 1 Optimization of reaction conditions<sup>a,g</sup>



Entry	Catalyst (mol%)	Solvent	Base (equiv.)	Time (h)	Yield <sup>b</sup> (%)
1	Eosin Y (2)	EtOH	KOH (0.5)	6	96
2	Eosin Y (2)	EtOH	KOH (0.2)	6	96
3	Rose bengal (2)	EtOH	KOH (0.2)	6	76
4	Fluorescein (2)	EtOH	KOH (0.2)	6	74
5	Nile red (2)	EtOH	KOH (0.2)	6	78
6	Perylene (2)	EtOH	KOH (0.2)	6	80
7	Rhodamine B (2)	EtOH	KOH (0.2)	6	83
8	Eosin Y (2)	DMSO	NaHCO <sub>3</sub> (0.5)	6	40
9	Eosin Y (2)	DMF	K <sub>2</sub> CO <sub>3</sub> (0.5)	6	82
10	Eosin Y (2)	Toluene	NaOH (0.5)	6	86
11	Eosin Y (1)	EtOH	KOH (0.2)	6	65
12	Eosin Y (3)	EtOH	KOH (0.2)	6	96
13	Eosin Y (2)	EtOH	KOH (0.2)	10	Traces <sup>c</sup>
14	—	EtOH	KOH (0.2)	10	n.d. <sup>d</sup>
15	Eosin Y (2)	EtOH	KOH (0.2)	10	60 <sup>e</sup>
16	Eosin Y (2)	EtOH	—	10	n.d. <sup>f</sup>

<sup>a</sup> Reaction conditions: **1a** (1.0 mmol), **2a** (1.0 mmol), catalyst (mol%), in 3 mL solvent irradiated using Luxeon Rebel high power green LEDs [18 W] at rt for 6–10 h. <sup>b</sup> Isolated yield of the pure product **3a**. <sup>c</sup> Reaction was performed in the dark. <sup>d</sup> Reaction was carried out without the catalyst. <sup>e</sup> 18 W CFL (compact fluorescent lamp, Philips) was used. <sup>f</sup> Reaction was carried out without the base. <sup>g</sup> After synthesis of **I**, further, reactions were carried out in presence of NaBH<sub>4</sub> without isolation.



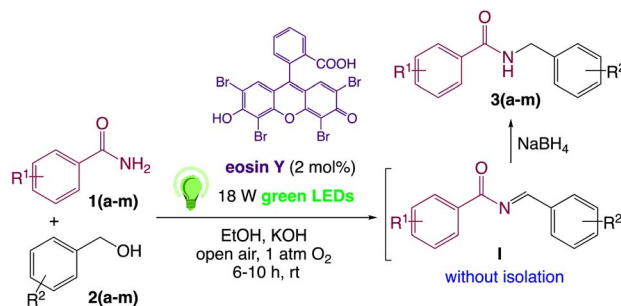
Scheme 2 Plausible mechanism for C–N coupling of amides with alcohols.<sup>60,61</sup>

versus 13, 14 and 16). Further, the reaction was carried out at room temperature (rt) in EtOH with 0.5 equivalents of a base and using 0.2 mol% of eosin Y for 6 hours (Table 1, entries 1 and 8–10). The use of KOH produced the *N*-monoalkylated product in the highest isolated yield (Table 1, entry 1). The quantity of KOH could be decreased to 0.2 equivalents, without any significant loss in yield (Table 1, entry 2). In any case, the product yields were unaffected by the longer reaction times. EtOH as a solvent was found to be superior for increasing yield and accelerating reaction times for the comparable product. In this approach, we reduce waste, tedious workup, and process costs.

We then turned our focus to investigating the adaptability of various substrates or anticipated reaction conditions as we continued to search for the best reaction conditions for our model reaction (Scheme 2). The scope of the present protocol across a range of benzamide and benzyl alcohol incorporating various substituents were studied. One important insight was that at the reaction conditions used, benzyl alcohol and benzamide with strong electron withdrawing groups as well as electron donating groups were well tolerated, and *N*-monoalkylated products were produced in good to excellent yields (Table 2). However, it was observed that benzyl alcohol and benzamide with electron-donating groups like methoxy and methyl at various positions exhibited improved reactivity and produced the corresponding products in good to excellent yields (3e, 3f and 3k). On the other hand, substrate containing electron-withdrawing groups, such as bromo and fluoro provided the corresponding products in good yields (3c, 3d and 3j). Further, it was also observed that the condensation reaction carried out between alkyl amide and alkyl alcohol then the yield of resultant product was found very low (3m).

On the basis of the observed reactivity and above investigations, even though the exact reaction mechanism is not clear, a plausible mechanistic pathway is depicted in Scheme 2. On absorption of visible light irradiation, the photo-excited eosin Y would induce an event of electron abstraction from benzyl alcohol 2a, whose oxidation potential might be significantly decreased under alkaline conditions, and thus gave rise to the highly active radical intermediate A and radical anion eosin Y. This radical anion eosin Y was able to be expediently oxidized by the molecular oxygen to go back to the ground state. The key

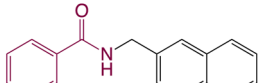
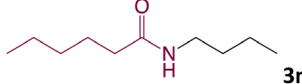
Table 2 Scope of the reaction

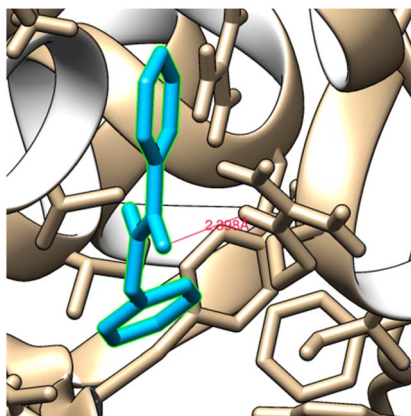


Entry	Product	Time/h	Yield
1		6	96
2		6	95
3		6	97
4		8	82
5		6	98
6		7	90
7		6	97
8		10	63
9		10	72
10		6	96
11		6	97



Table 2 (Contd.)

Entry	Product	Time/h	Yield	Reaction Scheme	
				1(a-m)	2(a-m)
12		6	97		
13		10	35		

Fig. 2 Ligand *N*-benzylbenzamide embedded in the active site of 1U3U protein.

intermediate, benzaldehyde **B**, would then be produced by further oxidizing and deprotonating the radical intermediate species **A** under the synergistic interactions of KOH and oxygen. Then, it went through a sequence of nucleophilic addition and dehydration reactions to produce the intermediate **I** without isolation, which further reduced<sup>59</sup> by NaBH<sub>4</sub> to give the desired product **3a**.

### 3. Molecular docking

It is usually known that drug design plays an important role in the pharma industry. This compound, referred to as a ligand, interacts with the appropriate protein that has been chosen using online drug target prediction Swiss ADME-

Table 3 Molecular docking and hydrogen bonding with centromere related protein inhibitors protein targets

Target molecule	<i>N</i> -Benzylbenzamide
Protein (PDB ID)	1U3U
No. of residues	3
Bond distance (Å)	2.39
Inhibition constant (micromolar)	4.46
Binding energy (kcal mol <sup>-1</sup> )	-7.3
Reference RMSD (Å)	9.34

Target prediction. By using Chimera 1.14 (ref. 62) and Autodock vina<sup>63</sup> software, *N*-benzylbenzamide molecule is docked with 1U3U protein belongs to oxidoreductase domain.<sup>64</sup> The best binding energy is shown -7.3 kcal mol<sup>-1</sup> is obtained as shown in Fig. 2 and the values are shown in Table 3. The low value of the binding energy indicates the bioactive nature of the molecule. The H-bond distance between bonded residue and ligand is 2.39 Å indicating the suitability of this ligand with given protein. The number of residue that contain by the protein 1U3U are 3 and KI value is 4.46.

### 4. Drug-likeness

In order to produce effective and efficient results in drug development, the structural property of the ligands plays a significant role for guidelines, described as drug-likeness. The calculations are based on a variety of rules, including QED, Lipinski's rule, MDDR-like rule, Veber rule, Ghose filter, and BBB rule, CMC-50 rule.<sup>65</sup> *N*-Benzylbenzamide and its derivatives demonstrate a wide range of activities that are applied to the drug-likeness rule and efficiency is obtained. For the title compound and its derivatives, the essential ADME parameters such as Hydrogen bond donors (HBD), Hydrogen bond acceptors (HBA), molar refractivity (MR), topological polar surface area (TPSA), blood–brain barrier penetration (BBB),  $\log k_p$ , and bioavailability score are calculated as given in Table 4. The values of HBD and HBA should be less than 10. Here, all of the molecule's values are less than 3. The maximum TPSA value is 140 Å<sup>2</sup>. For all target molecules, this value is between 29 and 39. The molar refractivity should also range from 40 to 130.<sup>66,67</sup> The MR value of *N*-Benzylbenzamide is 63.93 and the MR value for *N*-(4-methoxybenzyl)benzamide and *N*-[(4-fluorophenyl)methyl]benzamide is 70.42 and 63.88 respectively. Table 4 reveals that the GI absorption is high for all target molecules, the skin's permeability ( $\log k_p$ ) is between -6.01 and -6.21. The BBB is permeant available for all the target molecules, and the bioavailability score of *N*-benzylbenzamide and its derivative is the same as 0.55. The above comparison shows that the title compound (*N*-benzylbenzamide) and its derivatives are useful building blocks, frequently used in the synthesis of numerous bioactive components and medicines.

Table 4 ADME properties of *N*-benzylbenzamide and its derivatives<sup>a</sup>

ADME properties	Target molecule		
	<i>N</i> -Benzylbenzamide	<i>N</i> -(4-Methoxybenzyl)benzamide	<i>N</i> -[(4-Fluorophenyl)-methyl]benzamide
HBD	1	1	1
HBA	1	2	2
MR	63.93	70.42	63.88
TPSA A <sup>2</sup>	29.10	38.33	29.10
GI absorption	High	High	High
BBB permeant	Yes	Yes	Yes
CYP1A2 inhibitor	Yes	Yes	Yes
$\log k_p$ (cm s <sup>-1</sup> )	-6.01	-6.21	-6.04
Lipinski violations	0	0	0
Bioavailability score	0.55	0.55	0.55

<sup>a</sup> HBD – hydrogen bond donor, HBA – hydrogen bond acceptor, MR – molar refractivity, TPSA – topological polar surface area, GI – gastrointestinal, BBB – blood-brain barrier penetration and  $\log k_p$  – skin permeability.

## 5. Conclusions

In conclusion, we have established an effective synthetic protocol for *N*-monoalkylated product and its derivatives, *via* C–N bond formation by interaction of benzamide and benzyl alcohol with high reactivity and good selectivity. A variety of substrate amides were converted to the desired product with excellent yield along with low catalyst loading. This green synthetic pathway is superior to other synthetic process that uses harmful and corrosive chemicals. The range of substrates for visible light photoredox reaction is expanded by this synthesis. The proposed method also offers other benefits of green chemistry such high atom economy, shortened reaction time, and high efficiency. Molecular docking studies carried out on the 1U3U protein associated with the centromere protein inhibitor exhibited binding energy of -7.3 kcal mol<sup>-1</sup>, resulting its application in the medical field.

## Conflicts of interest

There are no conflicts to declare.

## References

- 1 D. Ma, S. Zhai, Y. Wang, A. Liu and C. Chen, *Front. Chem.*, 2019, **7**, 1–8.
- 2 C. L. Allen and J. M. J. Williams, *Chem. Soc. Rev.*, 2011, **40**, 3405–3415.
- 3 J. M. Humphrey and A. R. Chamberlin, *Chem. Rev.*, 1997, **97**, 2243–2266.
- 4 V. R. Pattabiraman and J. W. Bode, *Nature*, 2011, **480**, 471–479.
- 5 R. H. Crabtree, *Organometallics*, 2011, **30**, 17–19.
- 6 E. Emer, R. Sinisi, M. G. Capdevila, D. Petruzzello, F. D. Vincentiis and P. G. Cozzi, *Eur. J. Org. Chem.*, 2011, **2011**, 647–666.
- 7 G. Guillena, D. J. Ramón and M. Yus, *Chem. Rev.*, 2010, **110**, 1611–1641.
- 8 G. Guillena, D. J. Ramón and M. Yus, *Angew. Chem., Int. Ed.*, 2007, **46**, 2358–2364.
- 9 M. H. S. A. Hamid, P. A. Slatford and J. M. J. Williams, *Adv. Synth. Catal.*, 2007, **349**, 1555–1575.
- 10 M. Noji, T. Ohno, K. Fuji, N. Futaba, H. Tajima and K. Ishii, *J. Org. Chem.*, 2003, **68**, 9340–9347.
- 11 H. Qin, N. Yamagawa, S. Matsunaga and M. Shibasaki, *Angew. Chem., Int. Ed.*, 2007, **46**, 409–413.
- 12 S. Bojja, P. S. Reddy, M. A. Reddy and B. Neelima, *Tetrahedron Lett.*, 2007, **48**, 8174–8177.
- 13 A. J. A. Watson and J. M. J. Williams, *Science*, 2010, **329**, 635–636.
- 14 R. Blocher, C. Lamers, S. K. Wittmann, D. Merk, M. Hartmann, L. Weizel, O. Diehl, A. Bruggerhoff, M. Bo, A. Kaiser, T. Schader, T. G. Bel, M. Grundmann, C. Angioni, J. Heering, G. Geisslinger, M. Wurglics, E. Kostenis, B. B. Ne, D. Steinhilbe, M. S. Zsilavecz, A. S. Kahnt and E. Proschak, *J. Med. Chem.*, 2016, **59**(1), 61–81.
- 15 H. S. Baek, Y. D. Hong, C. S. Lee, H. S. Rho, S. S. Shin, Y. H. Park and Y. H. Joo, *ACS Med. Chem. Lett.*, 2012, **22**, 2110–2113.
- 16 H. Zhu, W. Li, W. Shuai, Y. Liu, L. Yang, Y. Tan, T. Zheng, H. Yao, J. Xu, Z. Zhu, D. H. Yang, Z. S. Chencand and S. Xu, *Eur. J. Med. Chem.*, 2021, **216**, 113316.
- 17 H. J. Shin, C. T. Oh, T. R. Kwon, H. S. Beak, Y. H. Joo, J. H. Kim, C. S. Lee, J. H. Lee, B. J. Kim, S. S. Shin and E. S. Park, *Int. J. Mol. Med.*, 2015, **36**, 1353–1360.
- 18 K. I. Fujita, A. Komatsubara and R. Yamaguchi, *Tetrahedron*, 2009, **65**, 3624–3828.
- 19 G. Jenner, *J. Mol. Catal.*, 1989, **55**, 241–246.
- 20 Y. Watanabe, T. Ohta and Y. Tsuji, *Bull. Chem. Soc. Jpn.*, 1983, **56**, 2647–2651.
- 21 G. C. Y. Choo, H. Miyamura and S. Kobayashi, *Chem. Sci.*, 2015, **6**, 1719–1727.
- 22 W. Yao, Y. Zhang, H. Zhu, C. Ge and D. Wang, *Chin. Chem. Lett.*, 2020, **31**, 701–705.



23 X. Cui, Y. Zhang, F. Shi and Y. Deng, *Chem.-Eur. J.*, 2011, **17**, 1021–1028.

24 A. M. Asencio, D. J. Ramón and M. Yus, *Tetrahedron*, 2011, **67**, 3140–3149.

25 A. J. A. Watson, A. C. Maxwell and J. M. J. Williams, *J. Org. Chem.*, 2011, **76**, 2328–2331.

26 C. Liu, S. Liao, Q. Li, S. Feng, Q. Sun, X. Yu and Q. Xu, *J. Org. Chem.*, 2011, **76**, 5759–5773.

27 F. Li, P. Qu, J. Ma, X. Zou and C. Sun, *ChemCatChem*, 2013, **5**, 2178–2182.

28 S. D. Tambe, M. S. Jadhav, R. S. Rohokale and U. A. Kshirsagar, *Eur. J. Org. Chem.*, 2018, 2117–2121.

29 Y. Zhou, J. Wang, Z. Gu, S. Wang, W. Zhu, J. L. Acenā, V. A. Soloshonok, K. Izawa and H. Liu, *Chem. Rev.*, 2016, **116**, 422–518.

30 T. Xu, C. W. Cheung and X. Hu, *Angew. Chem., Int. Ed.*, 2014, **53**, 4910–4914.

31 L. Buzzetti, G. E. M. Crisenza and P. Melchiorre, *Angew. Chem., Int. Ed.*, 2019, **58**, 3730–3747.

32 A. A. Soto, K. Kaastrup, S. Kim, K. Ugo-Beke and H. D. Sikes, *ACS Catal.*, 2018, **8**, 6394–6400.

33 L. Lin, X. Bai, X. Ye, X. Zhao, C. Tan and Z. Jiang, *Angew. Chem., Int. Ed.*, 2017, **56**, 13842–13846.

34 M. Majek and A. J. V. Wangelin, *Angew. Chem., Int. Ed.*, 2014, **53**, 1–6.

35 M. A. Ansari, D. Yadav, S. Soni, A. Srivastava and M. S. Singh, *J. Org. Chem.*, 2019, **84**, 5404–5412.

36 K. Wang, L. Meng and L. Wang, *J. Org. Chem.*, 2016, **81**, 7080–7087.

37 (a) K. Muralirajan, R. Kancherla and M. Rueping, *Angew. Chem., Int. Ed.*, 2018, **57**, 14787–14791; (b) A. G. Condie, J. C. Gonzalez-Gomez and C. R. J. Stephenson, *J. Am. Chem. Soc.*, 2010, **132**, 1464–1465; (c) S. W. Wang, J. Yu, Q. Y. Zhou, S. Y. Chen, Z. H. Xu and S. Tang, *ACS Sustainable Chem. Eng.*, 2019, **7**, 10154–10162; (d) X. Y. Yu, Q. Q. Zhao, J. Chen, W. J. Xiao and J. R. Chen, *Acc. Chem. Res.*, 2020, **53**, 1066–1083.

38 X. Lang, J. Zhao and X. Chen, *Angew. Chem., Int. Ed.*, 2016, **55**, 4697–4700.

39 R. S. Rohokale, B. Koenig and D. D. Dhavale, *J. Org. Chem.*, 2016, **81**, 7121–7126.

40 V. Srivastava, P. K. Singh and P. P. Singh, *Croat. Chem. Acta*, 2014, **87**, 91–95.

41 V. Srivastava, P. K. Singh and P. P. Singh, *Croat. Chem. Acta*, 2015, **88**, 59–65.

42 V. Srivastava, P. K. Singh and P. P. Singh, *Croat. Chem. Acta*, 2015, **88**, 227–233.

43 V. Srivastava, P. K. Singh and P. P. Singh, *Asian J. Chem.*, 2016, **28**, 2159–2638.

44 V. Srivastava, P. K. Singh and P. P. Singh, *Rev. Roum. Chim.*, 2016, **61**, 755–761.

45 V. Srivastava, P. K. Singh and P. P. Singh, *Croat. Chem. Acta*, 2017, **90**, 435–441.

46 V. Srivastava, P. K. Singh, S. Kanaujia and P. P. Singh, *New J. Chem.*, 2018, **42**, 688–691.

47 P. K. Singh, P. P. Singh and V. Srivastava, *Croat. Chem. Acta*, 2018, **91**, 383–387.

48 V. Srivastava, P. K. Singh and P. P. Singh, *Tetrahedron Lett.*, 2019, **60**, 40–43.

49 V. Srivastava, P. K. Singh and P. P. Singh, *Tetrahedron Lett.*, 2019, **60**, 1333–1336.

50 V. Srivastava, P. K. Singh and P. P. Singh, *Tetrahedron Lett.*, 2019, **60**, 151041–151638.

51 A. Srivastava, P. K. Singh, A. Ali, P. P. Singh and V. Srivastava, *RSC Adv.*, 2020, **10**, 39495–39508.

52 V. Srivastava, P. K. Singh and P. P. Singh, *Rev. Roum. Chim.*, 2020, **65**, 221–226.

53 V. Srivastava, P. K. Singh, A. Srivastava and P. P. Singh, *RSC Adv.*, 2021, **11**, 14251–14259.

54 P. P. Singh and V. Srivastava, *Org. Biomol. Chem.*, 2021, **19**, 313–321.

55 P. P. Singh, P. K. Singh, M. Z. Beg, A. Kashyap and V. Srivastava, *Synth. Commun.*, 2021, **51**(20), 3033–3058.

56 V. Srivastava, P. K. Singh, S. Tivari and P. P. Singh, *Org. Chem. Front.*, 2022, **9**, 1485–1507.

57 V. Srivastava, P. K. Singh and P. P. Singh, *J. Photochem. Photobiol. C*, 2022, **50**, 100488.

58 P. P. Singh and V. Srivastava, *RSC Adv.*, 2022, **12**, 18245–18265.

59 A. Rahman, A. Basha, N. Waheed and S. Ahmed, *Tetrahedron Lett.*, 1976, 219–222.

60 W. Yao, Y. Zhang, H. Zhu, C. Ge and D. Wang, *Chin. Chem. Lett.*, 2020, **53**, 701–705.

61 S. Kerdphon, X. Quan, V. S. Parihar and P. G. Andersson, *J. Org. Chem.*, 2015, **80**, 11529–11537.

62 D. R. Roy, R. Parthasarathi, B. Maity, V. Subramanian and P. K. Chattaraj, *Bioorg. Med. Chem.*, 2005, **13**, 3405–3412.

63 E. F. Pettersen, T. D. Goddard, C. C. Huang, G. S. Couch, D. M. Greenblatt, E. C. Meng and T. E. Ferrin, *J. Comput. Chem.*, 2005, **25**, 1605–1612.

64 B. J. Gibbons and T. D. Hurley, *Biochemistry*, 2004, **43**(39), 12555–12562.

65 H. Li, H. Wang, S. Kang, R. B. Silverman and T. L. Poulos, *Biochemistry*, 2016, **55**, 3702–3707.

66 A. Daina, O. Michielin and V. Zoete, *J. Chem. Inf. Model.*, 2014, **54**, 3284–3301.

67 C. A. Lipinski, F. Lombardo, B. W. Dominy and P. J. Feeney, *Adv. Drug Delivery Rev.*, 1997, **23**, 3–25.

